

Supplementary Information

Functional anatomy of an allosteric protein

Prasad Purohit, Shaweta Gupta, Snehal Jadey and Anthony Auerbach

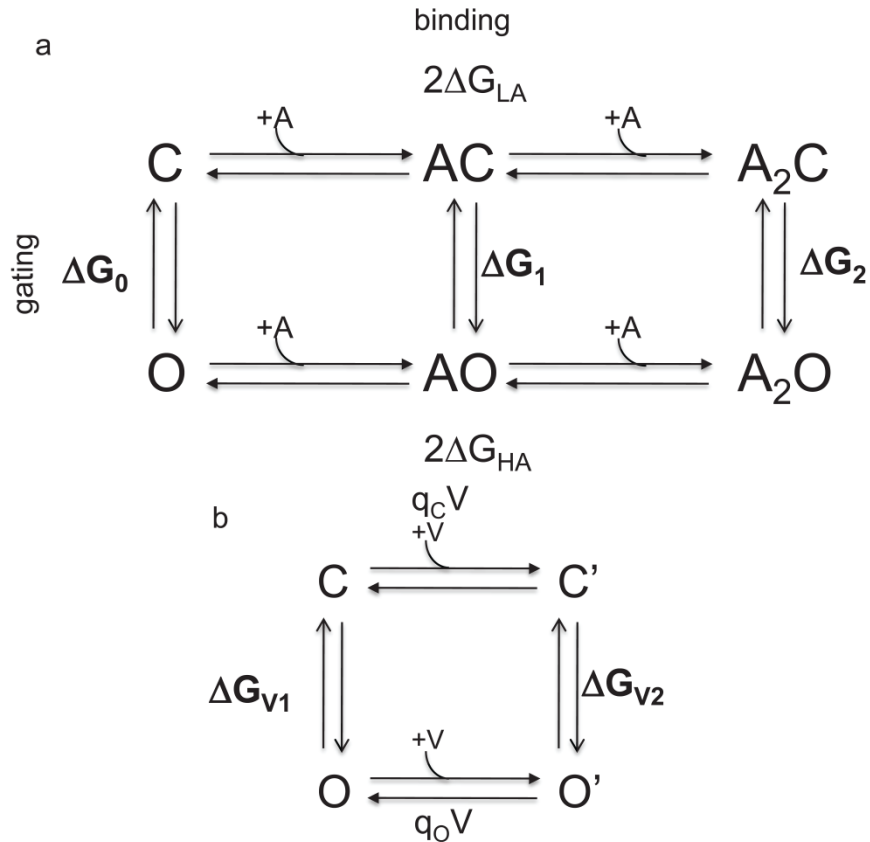
Department of Physiology and Biophysics, State University of New York at Buffalo, Buffalo NY

14214

Running Title: Energy maps of acetylcholine receptor gating

Supplementary Figures

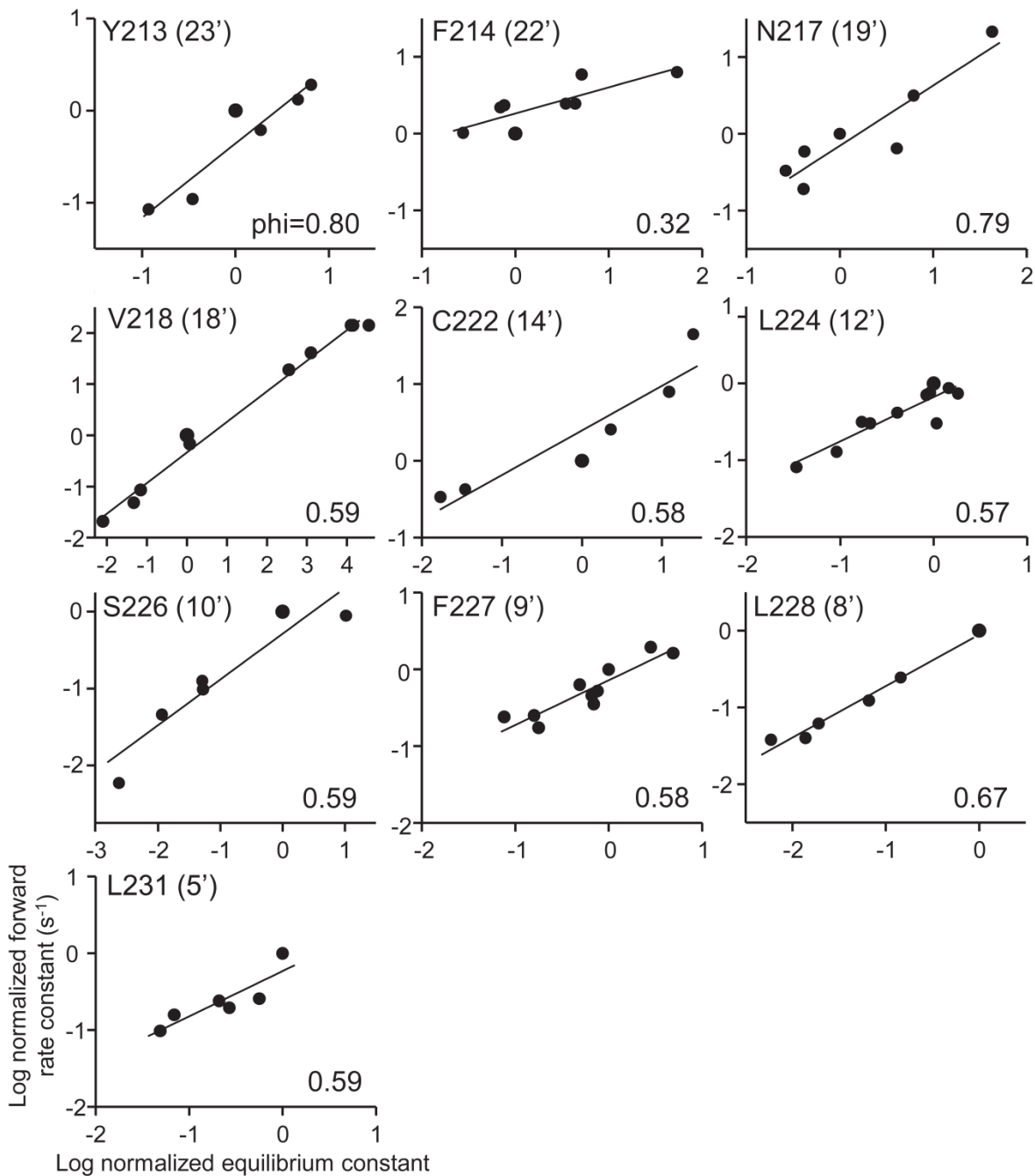
Supplementary Figure S1



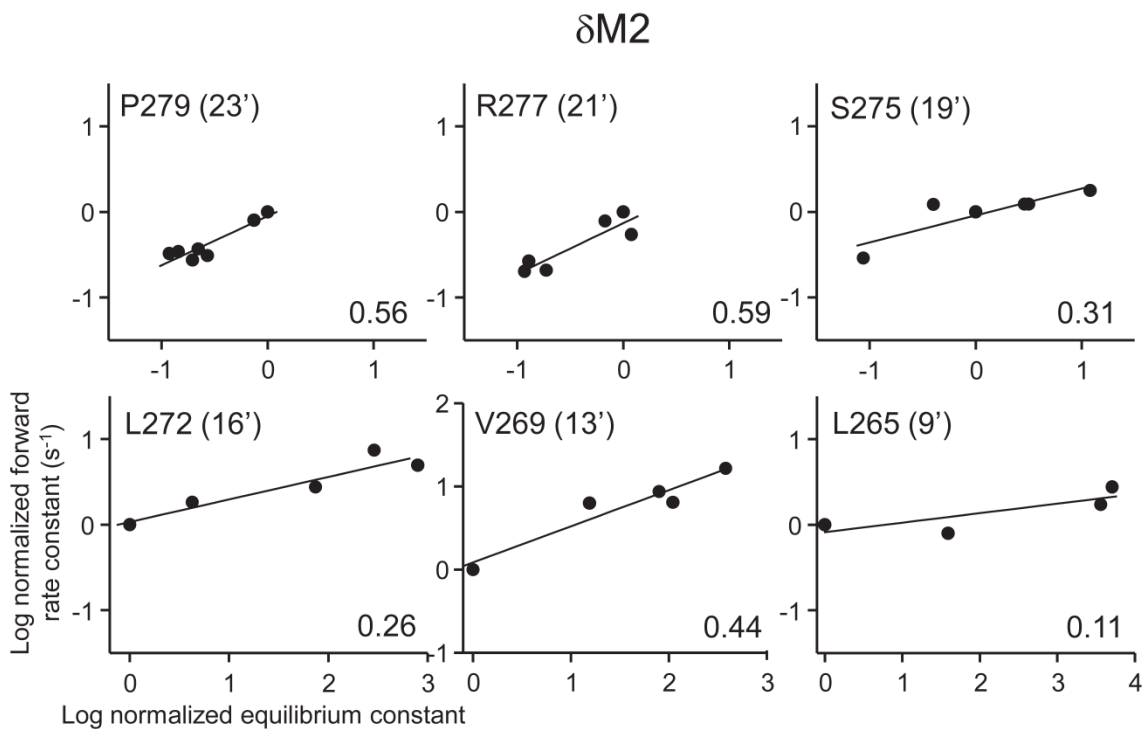
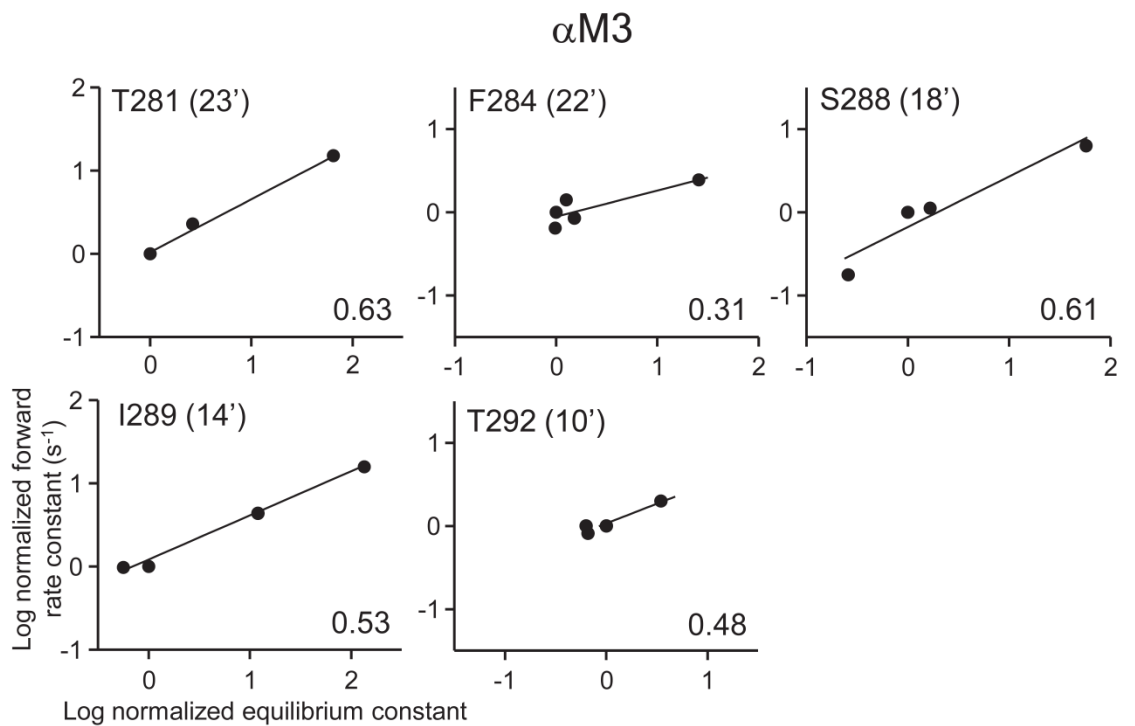
Supplementary Figure S1. Allosteric cycles. a. State model of a ligand-gated protein. The difference in free energy between the two ground states (O and C) is ΔG_n , where n is the number of bound agonists (A). ΔG_B is the difference in agonist binding energy, O (higher-affinity; ΔG_{HA}) vs. C (lower-affinity; ΔG_{LA}). $\Delta G_B (= \Delta G_{HA} - \Delta G_{LA})$ is the log of the ‘coupling constant’ and ΔG_0 is the log of the ‘allosteric constant’. ΔG_B^{ACh} is the same at the two adult mouse neuromuscular AChR neurotransmitter binding sites⁵⁴. From detailed balance, $\Delta G_2 = \Delta G_0 + 2\Delta G_B$. A mutation that changes ΔG_2 can do so by changing ΔG_0 , ΔG_B or both. **b.** State model of a voltage-gated protein. The environmental energy is voltage rather than ligand concentration. A change in voltage deposits different amounts of energy at the sensors ($=qV$, where q is charge and V is voltage) in C vs. O (analogous to ΔG_{LA} vs. ΔG_{HA}). The net energy from each sensor is $\Delta G_S = (q_O - q_C)V$ (analogous to ΔG_B). The vertical steps are the $C \leftrightarrow O$ gating transition at different voltages, with ground state energy differences ΔG_{V1} and ΔG_{V2} (analogous to ΔG_0 and ΔG_2). With 4 equivalent sensors, $\Delta G_{V2} = \Delta G_{V1} + 4\Delta G_S$. In this scheme voltage is deposited in the horizontal arrows and the sensor gating rearrangement (that generates the main gating current) occurs in the vertical arrows. A fast component of the gating current⁵⁵ may reflect the effect of voltage within the horizontal arrows.

Supplementary Figure S2a

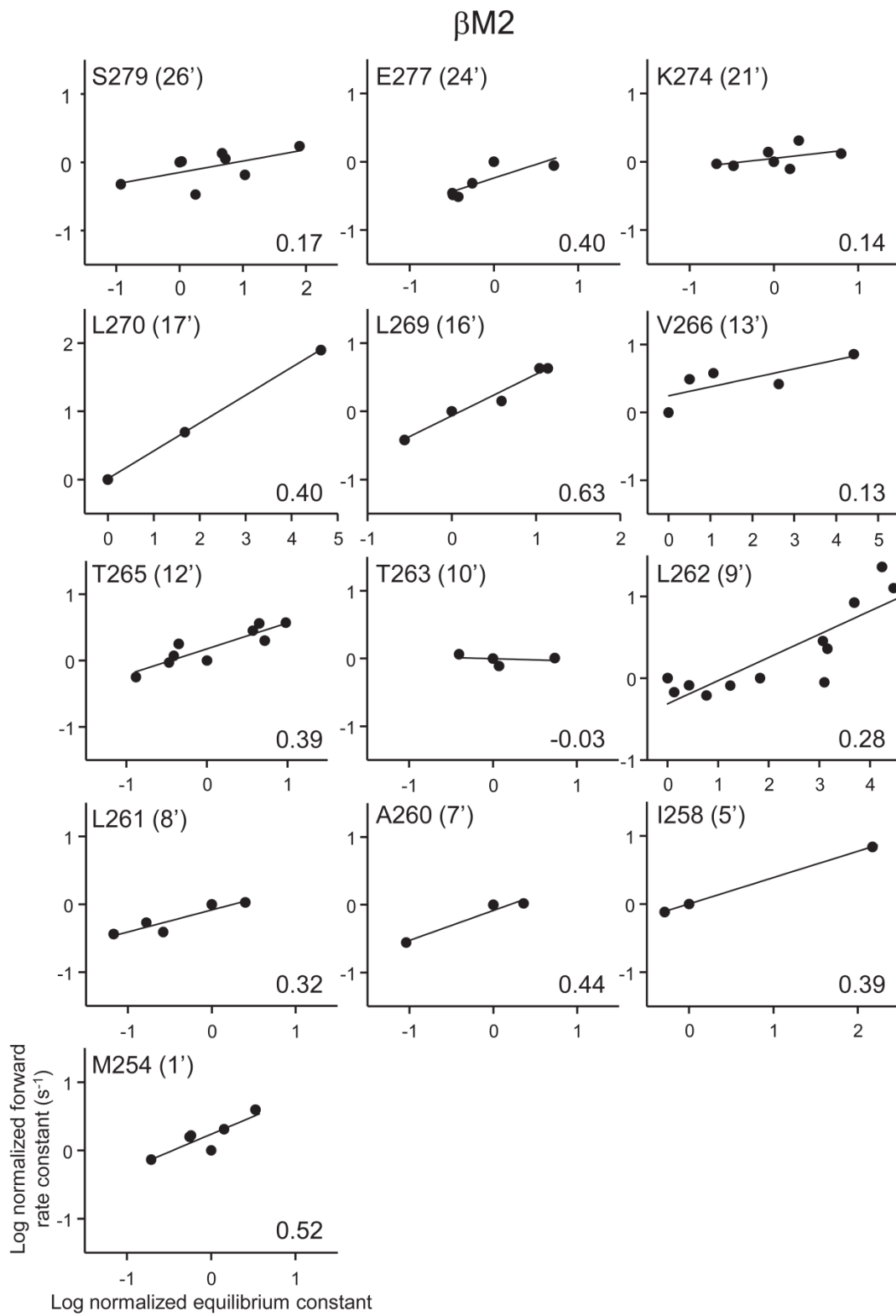
α M1



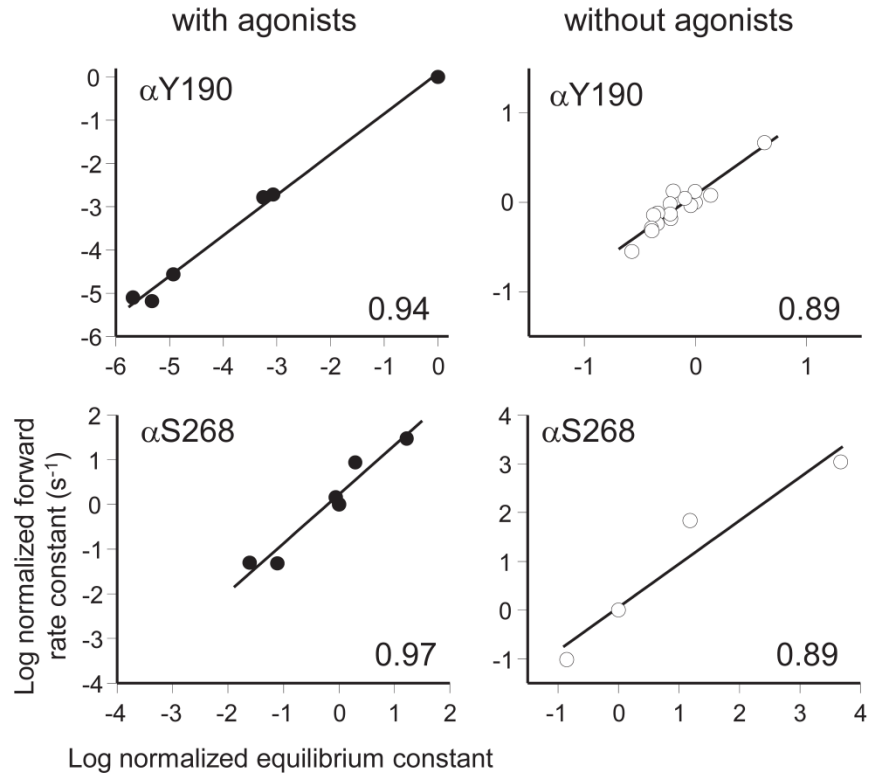
Supplementary Figure S2b



Supplementary Figure S2c

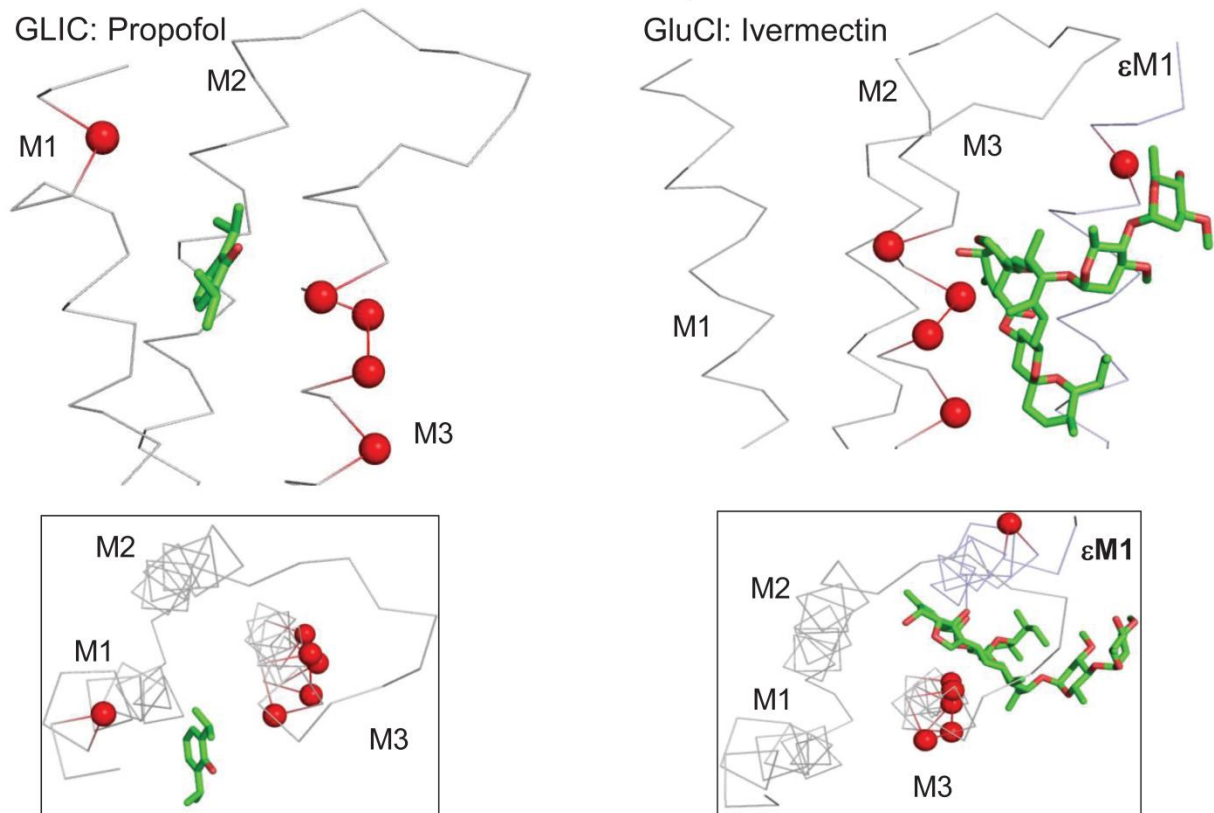


Supplementary Figure S2d



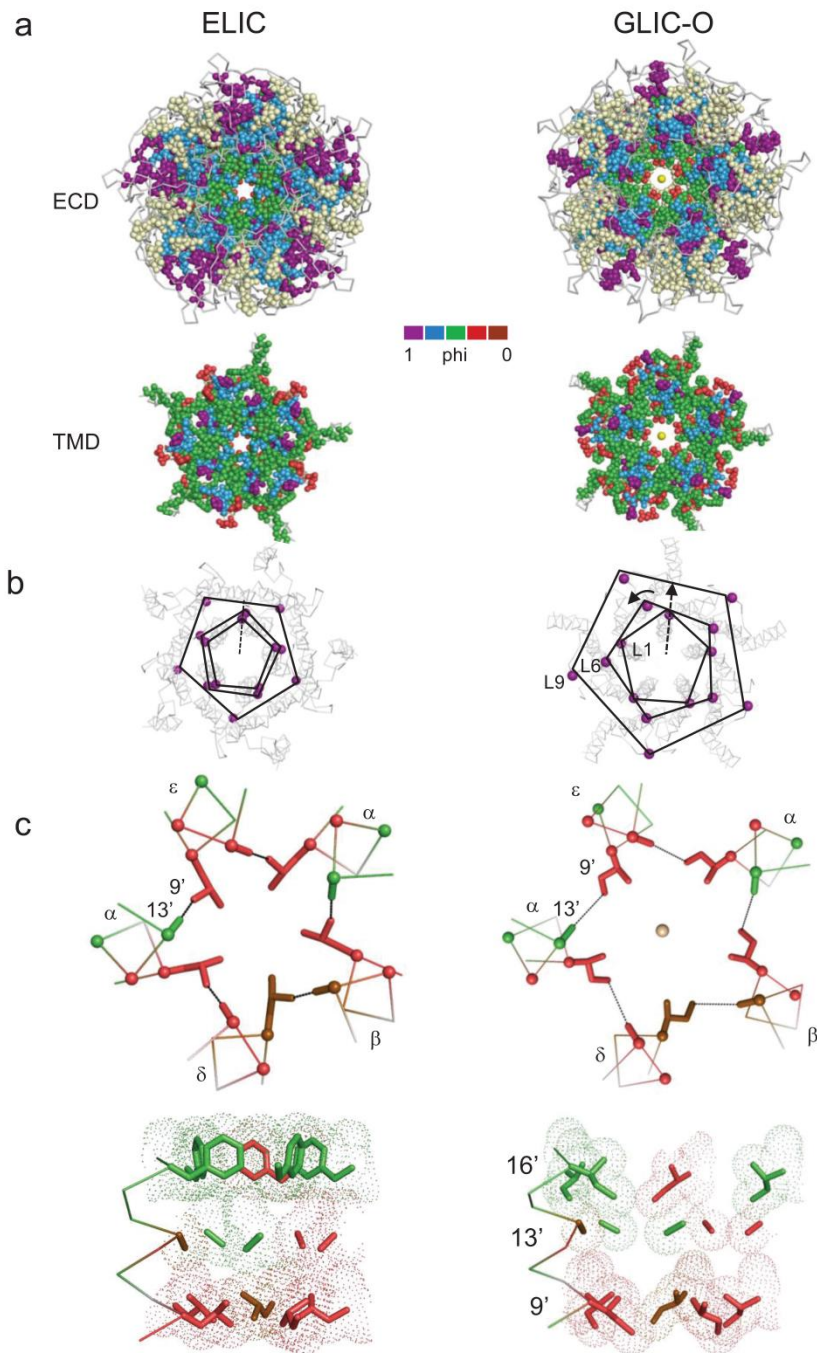
Supplementary Figure S2. R-E plots. Rate and equilibrium constants were estimated from single-channel current interval durations (Supplementary Table S3). Each panel is one amino acid position and each symbol is the mean of ≥ 3 measurements for one mutation of that amino acid. All values are normalized to the WT values (plotted at 0, 0). a-c. Gating with agonists at the binding sites. d. Phi values with and without agonists, for a binding site residue (α Y190)⁴⁵ and a residue in the gating linker (α S268)¹⁸. For α Y190, the larger range with agonists is from the contribution of the affinity change to the total energy of gating (ΔG_B ; see Supplementary Fig. S1).

Supplementary Figure S3



Supplementary Figure S3. Low-phi residues in the α TMD co-localize with ivermectin (GluCl) and propofol (GLIC) binding sites. The structures are from² and³.

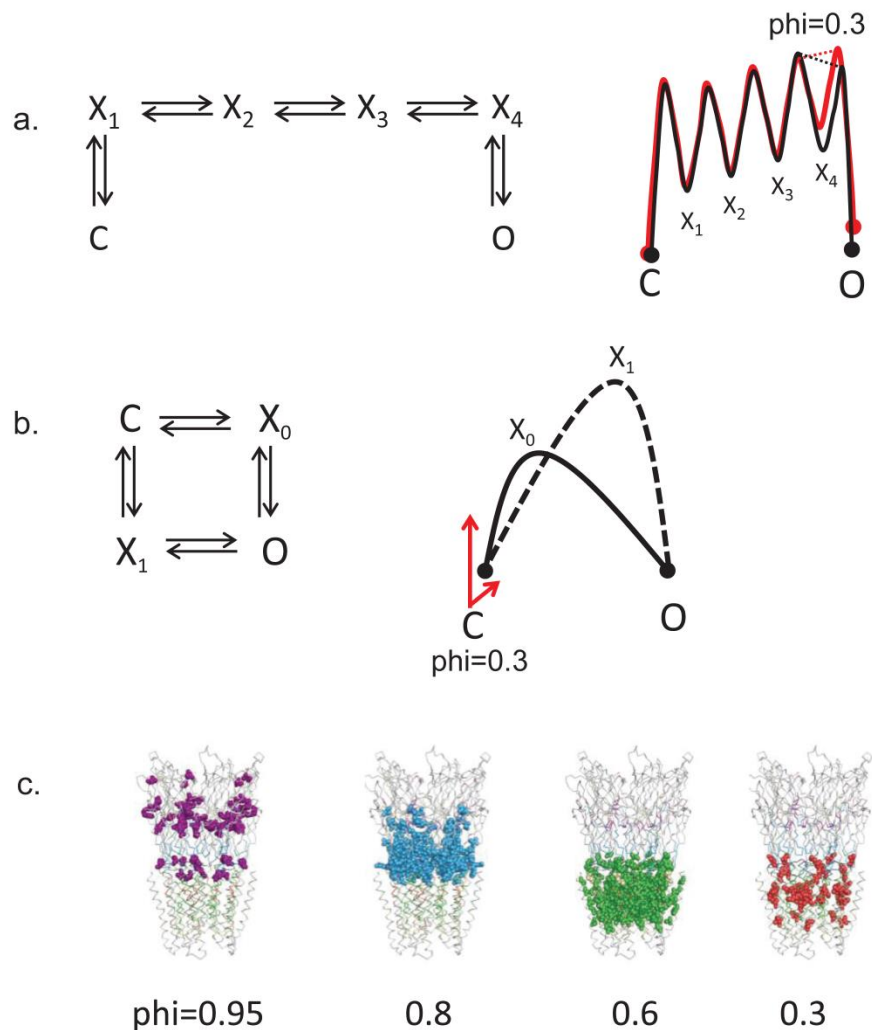
Supplementary Figure S4



Supplementary Figure S4. AChR α subunit phi values mapped onto non-conducting ELIC and ion-conducting GLIC structures. See Figs. 4 and 9 for a comparison between GLIC-LC1 and -O. a. Gating phi values of the ECD and TMD (view is from top). In ELIC \rightarrow GLIC, the ECD phi groups contract and the TMD groups expand. b. The high-phi residues have different orientations in ELIC vs. GLIC. All three positions (L1, L6 and L9) expand radially, and the

middle L6 ring is rotated anti-clockwise (ELIC→GLIC). c. Close-up views of the 9'-13'-16' gate region of M2.

Supplementary Figure S5



Supplementary Figure S5. Mechanisms for generating multiple, fractional phi values in an apparently one-step reaction. **a.** Serial model. Left, C and O are the gating ground states and each X is a brief, intermediate state in TSE. The 5 phi values arise from the 5 microscopic transitions, with phi giving the relative temporal sequence. Right, example energy landscape (black, WT; red, a phi=0.3 perturbation). Dotted lines show the change in the TSE barrier height profile. Perturbing the X₄ microwell yields phi=0.3 (X₁ yields phi=0.95, X₂ yields phi=0.80, and so on). **b.** Parallel model. X is a transition state with a phi value equal to 0 or 1 (subscript). A fractional phi value is the probability that the perturbed site takes the phi=1 pathway, which depends on the relative barrier height, the rate constant prefactor or both. Right, example energy landscape for phi=0.3 perturbation. Arrow length is proportional to path probability. **c.** Gating scenarios. In the serial scheme, the high-phi positions of the α subunit gating linkers and transmitter binding sites are the first to resettle (purple; C \leftrightarrow X₁). The gating movements of

amino acids at the binding sites result in an increased affinity for agonists. This is a local event that serves to stabilize A_2O relative to A_2C rather than to transfer significant energy towards the gate. Next, there is a twist of the ECD that perturbs many residues in all of the loops at the ECD-TMD interface and along subunit interfaces in the ECD (blue; $X_1 \leftrightarrow X_2$). Afterwards, the M2-M3 helices tilt to unpack the helix bundle, remove the M2-16' gate barrier and perturb the α M2-13' side chain (green; $X_2 \leftrightarrow X_3$). Still, the channel is non-conducting because most of the 9'-13' girdle remains intact. The α M2-13' destabilizes the rest of the girdle, which then expands to allow the extracellular and intracellular aqueous compartments to join and ion conduction to commence (red, $X_3 \leftrightarrow X_4$ and brown, $X_4 \leftrightarrow O$). In this scenario only X_4 and O are ion-conducting. In the parallel scheme, residues at the binding sites and α subunit gating linkers take the $\phi \sim 1$ path with a high probability and avoid the $\phi \sim 0$ path almost completely (purple). As above, the gating movements of amino acids at the binding sites result in an increased affinity for agonists that stabilize A_2O relative to A_2C locally rather than to transfer significant energy towards the gate. At the same time, most residues in the ECD take the low ϕ path with $\sim 20\%$ probability (blue), those that face the TMD bundle core with a $\sim 40\%$ probability (green) and most of those at the hydrophobic girdle (and in other scattered regions of the TMD) with a $\sim 70\%$ probability (red). In this scheme all residue motions could be approximately synchronous, with no time correlation associated with ϕ . The stable, ion-conducting O ensemble is achieved when all residues have traversed the barriers of both reaction pathways. The serial and parallel mechanisms for AChR gating cannot be distinguished by ϕ analysis, where kinetic scheme CXX and XCX are equivalent. Serial and parallel mechanisms are not exclusive.

Supplementary Table S1. Mutational changes in un- vs. di-liganded gating energy.

The values are plotted graphically in Fig. 1b. The change in the A₂O vs. A₂C energy difference ($\Delta\Delta G_2$) was estimated from single-channel current interval durations, using a WT background and with agonists at the binding sites. The change in the O vs. C energy difference ($\Delta\Delta G_0$) was estimated without any agonist, using background mutations that only changed ΔG_0 (to facilitate the measurements).

Construct	$\Delta\Delta G_0$ (kcal/mol)	$\Delta\Delta G_2$ (kcal/mol)
α N217K ^a	-2.2	-2.3
T	-1.1	-1.1
F	-0.8	-0.9
Q	0.5	0.4
E	0.5	0.8
A	0.8	0.3
α V218Y ^a	-5.6	-5.6
S	-0.1	0.9
α L279W ^b	-3.07	-2.98
α V283W ^b	-0.92	-1.4
α I260M ^c	1.2	0.83
S ^d	2.7	2.25
A ^e	3.8	3.43
α E262G ^c	-1.2	-1.77
L ^c	1	1.06
α P265K ^e	4.4	4.21
α S268E ^f	-3.9	-2.81
D ^g	-1.6	-1.67
L ^h	1.2	2.2
α S269I ^b	-2.63	-2.8
α P272A ^b	-2.76	-3.23
α L410F ^a	-0.2	-0.38
A ^a	-0.8	-0.99
α C418F ^c	-1.8	-1.5
Y ^c	-2.1	-2.52
W ^b	-3.1	-2.8
α T422V ⁱ	2.1	1.84
α F426A ^a	-1.5	-1.62
W ^a	-0.5	-0.75

$\delta V269L^a$	-1.2	-1.56
C^a	-2.11	-2.5
A^a	-3.78	-3.41
$\varepsilon V265M^a$	-2.15	-2.01
A^a	-3.04	-3.25
G^a	-4.58	-4.74
N^a	-5.33	-5.69
$\varepsilon S450W^b$	-1.14	-1.35
$\varepsilon S450A^b$	-1.33	-1.68

Unliganded gating backgrounds: ^a $\alpha(D97A+Y127F+S269I)$; ^b $\beta L262S+\delta L265S$; ^c $\alpha(D97A+Y127F+S269I+W149F)$; ^d $\alpha(D97A+Y127F+S269I)+\delta V269C$; ^e $\alpha(D97A+Y127F+S269I+C418W)$; ^f $\delta I43Q$, ^g $\alpha(D97A+Y127F)$; ^h $\alpha(D97A+Y127F)+\delta V269C$.

Supplementary Table S2. Newly-studied mutants (AChR numbering)

Subunit -domain	Position	Mutants	N
α -ECD	T52	VAFY	4
	W86	F	1
	S126	EFYW	4
α -M1	L212	GCVVHA	6
	Y213	SACMF	5
	F214	LSMTCWA	7
	I215	MFSLNAKVDP	10
	I216	YLMFSI	6
	N217	KTFQEA	6
	V218	YFMSCA	6
	I219	KNVSFMA	7
	I220	YAMTL	5
	P221	AGSLCTVRFY	10
	C222	WAVTFL	6
	L223	NMECGATY	8
	L224	EMSFACTGVN	10
	F225	SALVI	5
	S226	FCNLM	5
	F227	SNAPCIWMV	9
	L228	WVCTA	5
	T229	ACS	3
	S230	CFI	3
	L231	YIAQS	5
	V232	ATC	3
	F233	ASY	3
	Y234	FCSA	4
	L235	IAC	3
	P236	ACGSF	5
	T237	LCDA	4
	D238	AEC	3
S239	CFA	3	
G240	SCA	3	
α -M3	M278	LCA	3
	T281	LC	2
	M282	LW	2
	F284	WLCA	4
	T285	WALC	4
	S288	LVM	3
	I289	WYS	3
	T292	LAC	3
I296	LAC	3	

	N297	M	1
	H299	ACWL	4
α -M4	V413	KMPQ	4
	V417	KT	2
	I420	CMNT	4
	L423	ASW	3
	A424	CLPRT	5
	V425	LPRW	4
	A427	LNRW	4
	G428	AER	3
β -M2	M254	PIVLH	5
	G255	AHLVWY	6
	L256	DVHKRF	6
	S257	DAHRVW	6
	I258	VFKT	4
	F259	YAEGV	5
	A260	HVDFWS	6
	L261	AFWHINRST	9
	L262	IAMENQDTSVW	11
	T263	NAHDR	5
	L264	DFHRTW	6
	T265	DNAHR	5
	V266	LMADR	5
	F267	DRHA	4
	L268	ADHRSV	6
	L269	ANKDRH	6
	L270	ADKR	4
	L271	DHAR	4
	A272	FWRDHK	6
	D273	AHFERW	6
	K274	RHFAWD	6
	V275	HDARL	5
	P276	HKESARD	7
	E277	FRHMW	5
	T278	ADFHLQWY	8
	S279	WAKTRHD	7
	L280	RAKHDW	6
δ -M2	S258	GWAECDN	7
	V259	DMQTY	5
	A260	EFITV	5
	I261	GFEY AEMT	8
	S262	ECFAKQCGL	9
	L264	TGCDVR	6
	L265	CDQ PMWV	7
	F270	ARVSNL	6

	L272	CASQ ERYFIM	10
	I274	ECWFAMGKRSY	11
	S275	DGAYF CEGIRKT	12
	K276	YGDSAEGCFIRT	12
	R277	YAEIG CFSTK	10
	L278	RIEDFCKSTY	10
	P279	KFCERY	10
	A280	FIYKRCESDGT	11
	T281	RWSCAEFIMPQ	11
	S282	AEQTFCEIMPR	11
	M283	RECFIS	6

N is number of side chains at each position.

Supplementary Table S3. Phi and range values (all AChR mutants)

α AChR	#	ELIC	#	GLIC	#	GluCl	#	Phi	SE	range	Citation ¹
R	20	D	4	P	7	R	19	-	-	0.6	28
V	29	V	12	L	16	V	28	-	-	0.3	28
V	31	V	14	V	18	V	30	-	-	0.4	28
L	35	I	18	I	22	M	34	-	-	0.3	28
L	40	I	23	C	27	I	39	-	-	0.8	28
E	45	T	28	D	32	V	44	0.8	0.06	5.1	43
V	46	L	29	K	33	V	45	0.81	0.05	5.4	28
N	47	E	30	A	34	N	46	0.81	0.05	5.4	28
Q	48	Q	31	E	35	M	47	0.81	0.05	5.4	28
I	49	T	32	T	36	E	48	0.71	0.13	2.3	41
T	52	V	35	V	39	A	51	1.0	0.12	1.1	
V	54	G	37	A	41	L	53	-	-	0.4	28
R	55	Y	38	F	42	T	54	-	-	0.3	28
L	56	I	39	L	43	L	55	-	-	0.3	28
L	65	R	47	L	52	L	64	-	-	0.1	28
W	86	W	72	W	72	W	86	-	-	2.0	
P	88	P	74	P	74	P	88	-	-	NF	28
D	89	A	75	E	75	D	89	-	-	NF	28
Y	93	I	79	V	78	P	93	0.88	0.05	2.0	45
N	94	N	80	N	79	N	94	0.86	0.03	3.8	41
A	96	V	82	E	81	K	96	0.79	0.05	6.9	41
D	97	G	83	N	82	Q	97	0.93	0.04	3.0	46
L	110	L	94	V	94	I	112	-	-	0.2	28
G	114	G	98	G	98	G	116	-	-	NF	28
I	116	V	100	V	100	V	118	-	-	0.0	28
P	120	A	104	E	104	V	122	-	-	0.0	28
A	122	F	106	F	106	I	124	-	-	0.7	28
S	126	F	110	V	110	L	128	0.79	0.04	3.3	
Y	127	S	111	L	111	S	129	0.77	0.02	5.0	47
V	132	F	116	F	116	L	134	0.75	0.08	4.7	20
H	134	L	118	R	118	Y	136	0.71	0.03	1.4	20
F	135	F	119	Y	119	Y	137	0.75	0.12	1.7	20
P	136	P	120	P	120	P	138	-	-	NF	20
F	137	F	121	F	121	M	139	0.78	0.03	4.0	28
D	138	D	122	D	122	D	140	0.78	0.03	4.0	28
Q	140	Q	124	Q	124	Q	142	0.78	0.03	4.0	28
N	141	Q	125	T	125	Q	143	0.78	0.03	4.0	28
I	143	V	127	H	127	S	145	0.78	0.03	0.1	28
M	144	L	128	I	128	I	146	0.84	0.06	1.1	28
K	145	E	129	Y	129	D	147	0.96	0.04	3.3	47
L	146	L	130	L	130	L	148	-	-		28
G	147	E	131	I	131	A	149	0.86	0.03		48

W	149	F	133	R	133	Y	151	0.97	0.06	4.0	45
G	153	N	138	T	137	T	155	0.96	0.06	3.1	48
G	174	D	158	T	158	P	179	0.82	0.10	1.6	42
E	175	E	159	G	159	S	180	0.52	0.06	2.1	42
W	176	W	160	W	160	F	181	0.85	0.09	1.2	42
Y	190	Y	175	F	174	T	195	0.89	0.10	1.6	45
Y	198	F	188	E	181	Y	200	1.00	0.04	1.4	45
R	209	R	199	R	192	R	211	0.72	0.15	2.5	43
L	210	N	200	Q	193	E	212	0.35	0.12	2.3	43
P	211	P	201	Y	194	F	213	-	-	0.5	43
L	212	S	202	F	195	S	214	-	-	1.2	
Y	213	Y	203	S	196	F	215	0.80	0.14	2.4	
F	214	Y	204	Y	197	Y	216	0.32	0.09	3.2	
I	215	L	205	I	198	L	217	-	-	1.0	
I	216	W	206	P	199	L	218	-	-	0.7	
N	217	S	207	N	200	Q	219	0.79	0.15	3.0	
V	218	F	208	I	201	L	220	0.59	0.02	8.5	
I	219	I	209	I	202	Y	221	-	-	1.2	
I	220	L	210	L	203	I	222	-	-	0.6	
P	221	P	211	P	204	P	223	-	-	-	
C	222	L	212	P	205	S	224	0.58	0.10	4.3	
L	223	G	213	M	206	C	225	-	-	1.4	
L	224	L	214	F	207	M	226	0.57	0.08	1.8	
F	225	I	215	L	208	L	227	0.57	0.07	3.3	
S	226	I	216	L	209	V	228	0.59	0.10	4.0	
F	227	A	217	F	210	I	229	0.58	0.09	2.4	
L	228	A	218	I	211	V	230	0.67	0.05	3.0	
T	229	S	219	S	212	S	231	-	-	0.4	
S	230	W	220	W	213	W	232	-	-	1.2	
L	231	S	221	T	214	V	233	0.59	0.15	1.8	
V	232	V	222	A	215	S	234	-	-	0.5	
F	233	F	223	F	216	F	235	-	-	0.5	
Y	234	W	224	W	217	W	236	-	-	0.8	
L	235	L	225	S	218	F	237	-	-	1.3	
P	236	E	226	T	219	D	238	-	-	NF	
T	237	S	227	S	220	R	239	-	-	1.1	
D	238	F	228	Y	221	T	240	-	-	0.3	
S	239	gap	gap	gap	gap	A	241	-	-	0.6	
G	240	gap	gap	gap	gap	I	242	-	-	0.3	
T	244	Q	233		226		247	-	-	0.0	22
L	245	T	234	L	227	L	248	0.61	0.02	2.0	22
S	246	S	235	V	228	G	249	0.63	0.13	2.9	22
I	247	F	236		229		250	-	-	0.0	22
S	248	T	237	S	230	T	251	0.65	0.15	1.2	22
V	249	L	238	T	231	T	252	0.50	0.06	2.5	22

L	250	M	239	L	232	L	253	0.66	0.04	1.1	22
L	251	L	240	I	233	L	254	0.26	0.04	3.4	22
S	252	T	241	V	234	T	255	-	-	0.3	22
L	253	V	242	H	235	M	256	0.55	0.08	3.2	22
T	254	V	243	I	236	T	257	0.35	0.09	3.9	22
V	255	A	244	A	237	A	258	0.52	0.01	5.5	22
F	256	Y	245	F	238	Q	259	0.67	0.09	3.3	22
L	257	A	246	N	239	S	260	0.62	0.15	3.7	22
L	258	F	247	I	240	A	261	0.61	0.09	3.3	22
V	259	Y	248	L	241	G	262	0.61	0.04	2.6	49
I	260	T	249	V	242	I	263	0.89	0.04	3.4	18
V	261	S	250	E	243	N	264	0.78	0.11	4.1	18
E	262	N	251	T	244	S	265	0.82	0.15	2.8	18
L	263	I	252	N	245	Q	266	0.66	0.12	3.3	18
I	264	L	253	I	246	L	267	0.78	0.15	4.6	18
P	265	P	254	P	247	P	268	0.90	0.10	5.4	18
S	266	R	255	K	248	P	269	0.64	0.13	4.1	18
T	267	L	256	T	249	V	270	0.71	0.09	2.9	18
S	268	P	257	P	250	S	271	0.97	0.11	5.0	18
S	269	Y	258	Y	251	Y	272	0.61	0.06	2.8	49
A	270	T(g)	259	M(g)	252	I(g)	273	0.65	0.07	3.0	20
V	271							-	-	0.4	20
P	272	T	260	T	253	K	274	0.62	0.05	5.5	20
L	273	V	261	Y	254	A	275	-	-	0.8	20
I	274	I	262	T	255	I	276	0.62	0.04	4.5	20
G	275	D	263	G	256	D	277	0.65	0.06	2.6	20
K	276	Q	264	A	257	V	278	-	-	1.0	20
Y	277	M	265	I	258	W	279	0.34	0.11	3.0	50
M	278	I	266	I	259	I	280	-	-	1.2	
L	279	I	267	F	260	G	281	0.27	0.02	3.0	50
F	280	A	268	M	261	A	282	0.30	-	0.8	50
T	281	G	269	I	262	C	283	0.63	0.05	2.5	
M	282	Y	270	Y	263	M	284	-	-	0.6	
V	283	G	271	L	264	T	285	0.29	0.02	1.4	50
F	284	S	272	F	265	F	286	0.32	0.11	1.9	
V	285	I	273	Y	266	I	287	-	-	-	
I	286	F	274	F	267	F	288	-	-	-	
A	287	A	275	V	268	C	289	-	-	-	
S	288	A	276	A	269	A	290	0.61	0.12	2.4	
I	289	I	277	V	270	L	291	0.53	0.04	2.9	
I	290	L	278	I	271	L	292	0.31	0.02	1.1	50
I	291	L	279	E	272	E	293	-	-	-	
T	292	I	280	V	273	F	294	0.48	0.09	1.0	
V	293	I	281	T	274	A	295	-	-	0.2	50
I	294	F	282	V	275	L	296	-	-	0.3	50

V	295	A	283	Q	276	V	297	-	-	-	
I	296	H	284	H	277	N	298	-	-	0.8	
N	297	H	285	Y	278	H	299	-	-	0.2	50
T	298	R	286	L	279	I	300	-	-	-	
H	299	Q	287	K	280	A	301	-	-	0.9	
L	410	C	300	S	295	S	319	0.54	0.04	1.0	51
V	413	A	303	A	298	L	322	-	-	0.0	
M	415	P	305	P	300	P	324	0.57	0.09	0.6	51
V	417	G	307	V	302	L	326	-	-	0.0	
C	418	F	308	L	303	F	327	0.50	0.01	2.8	51
I	420	A	310	L	305	V	329	-	-	0.0	
T	422	G	312	N	307	N	331	0.54	0.04	1.8	51
L	423	C	313	I	308	I	332	-	-	0.0	
A	424	V	314	I	309	L	333	-	-	0.0	
F	426	V	316	A	311	W	335	0.56	0.03	1.6	51
A	427	I	317	F	312	S	336	-	-	0.0	
G	428	R	318	L	313	R	337	-	-	0.0	
R	429	G	319	F	314	F	338	-	-	0.0	
βAChR	#	ELIC	#	GLIC	#	GluCl	#	Phi	SE	range	
L	280	Y	258	Y	251	Y	272	-	-	0.7	
S	279	P	257	P	250	S	271	0.17	0.09	2.4	
T	278	L	256	T	249	V	270	-	-	0	
E	277	R	255	K	248	P	269	0.40	0.14	1	
P	276	P	254	P	247	P	268	-	-	0.7	
V	275	L	253	I	246	L	267	-	-	0.3	
K	274	I	252	N	245	Q	266	0.14	0.12	1.1	
D	273	N	251	T	244	S	265	-	-	0	
A	272	S	250	E	243	N	264	-	-	0.5	
L	271	T	249	V	242	I	263	-	-	0	
L	270	Y	248	L	241	G	262	0.40	0.00	6.3	
L	269	F	247	I	240	A	261	0.63	0.08	3.8	
L	268	A	246	N	239	S	260	-	-	1.2	
F	267	Y	245	F	238	Q	259	-	-	0.35	
V	266	A	244	A	237	A	258	0.13	0.06	6	
T	265	V	243	I	236	T	257	0.39	0.07	1.3	
L	264	V	242	H	235	M	256	-	-	0	
T	263	T	241	V	234	T	255	0.00	0.11	1.6	
A	262	L	240	I	233	L	254	0.30	0.06	5.9	
L	261	M	239	L	232	L	253	0.32	0.08	2.6	
A	260	L	238	T	231	T	252	0.44	0.10	1.9	
F	259	T	237	S	230	T	251	-	-	1.3	
I	258	F	236	V	229	V	250	-	-	2.1	
S	257	S	235	V	228	G	249	-	-	0.3	
L	256	T	234	L	227	L	248	-	-	0.5	
G	255	Q	233	T	226	T	247	-	-	0	

M	254	L	232	V	225	V	246	-	-	0.7	
T	464	G	312	N	307	N	331	0.17	0.05	1.0	51
δAChR	#	ELIC	#	GLIC	#	GluCl	#	Phi	SE	range	
M	283	Y	258	Y	251	Y	272	-	-	0.8	
S	282	P	257	P	250	S	271	-	-	0.3	
T	281	L	256	T	249	V	270	-	-	0.9	
A	280	R	255	K	248	P	269	-	-	0.2	
P	279	P	254	P	247	P	268	0.56	0.15	1.4	
L	278	L	253	I	246	L	267	-	-	0.7	
R	277	I	252	N	245	Q	266	0.59	0.14	1.3	
K	276	N	251	T	244	S	265	-	-	1.5	
S	275	S	250	E	243	N	264	0.31	0.10	3.0	23
I	274	T	249	V	242	I	263	-	-	0.7	
L	273	Y	248	L	241	G	262	0.37	0.03	2.9	23
L	272	F	247	I	240	A	261	0.26	0.06	4.0	
L	271	A	246	N	239	S	260	-	-	1.0	
F	270	Y	245	F	238	Q	259	-	-	1.0	
V	269	A	244	A	237	A	258	0.44	0.10	4.1	
S	268	V	243	I	236	T	257	0.28	0.02	3.8	
Q	267	V	242	H	235	M	256	-	-	1.1	
A	266	T	241	V	234	T	255	-0.05	0.03	1.2	
L	265	L	240	I	233	L	254	0.11	0.06	5.1	23
L	264	M	239	L	232	L	253	-	-	1.0	
V	263	L	238	T	231	T	252	-0.1	0.13	1.0	23
S	262	T	237	S	230	T	251	-	-	0.6	
I	261	F	236	V	229	V	250	-0.05	0.03	0.7	23
A	260	S	235	V	228	G	249	-	-	0.8	
V	259	T	234	L	227	L	248	-	-	1.0	
S	258	Q	233	T	226	T	247	-	-	2.1	23
T	257	L	232	V	225	V	246	-	-	-	
I	43	Y	24	Y	28	S	40	0.86	0.10	2.8	47
W	57	Y	38	F	42	T	54	0.94	0.11	1.7	52
P	123	R	105	R	105	R	123	0.90	0.09	4.4	14
εAChR	#	ELIC	#	GLIC	#	GluCl	#	Phi	SE	range	
I	279	Y	258	Y	251	Y	272	-	-	-	16
S	278	P	257	P	250	S	271	-	-	0.8	16
T	277	L	256	T	249	V	270	-	-	0.8	16
E	276	R	255	K	248	P	269	0.56	0.12	1.6	16
P	275	P	254	P	247	P	268	0.51	0.10	1.6	16
I	274	L	253	I	246	L	267	-	-	1.2	16
K	273	I	252	N	245	Q	266	-	-	1.1	16
Q	272	N	251	T	244	S	265	-	-	1.2	16
A	271	S	250	E	243	N	264	-	-	1.3	16
I	270	T	249	V	242	I	263	-	-	1.1	16
L	269	Y	248	L	241	G	262	0.52	0.06	3.1	16

F	268	F	247	I	240	A	261	0.51	0.06	3.8	16
L	267	A	246	N	239	S	260	-	-	1.2	16
F	266	Y	245	F	238	Q	259	0.56	0.07	1.9	16
V	265	A	244	A	237	A	258	0.34	0.07	5.7	16
T	264	V	243	I	236	T	257	0.26	0.08	5.3	16
Q	263	V	242	H	235	M	256	0.55	0.04	1.9	16
A	262	T	241	V	234	T	255	0.59	0.05	1.7	16
L	261	L	240	I	233	L	254	0.37	0.10	4.2	16
L	260	M	239	L	232	L	253	0.50	0.10	2.8	16
V	259	L	238	T	231	T	252	0.58	0.10	1.7	16
N	258	T	237	S	230	T	251	-	-	1.2	16
I	257	F	236	V	229	V	250	0.33	0.08	2.5	16
S	256	S	235	V	228	G	249	-	-	1.1	16
V	255	T	234	L	227	L	248	0.56	0.06	1.4	16
T	254	Q	233	T	226	T	247	-	-	0.7	16
C	253	L	232	V	225	V	246	-	-	-	16
W	55	Y	38	F	42	T	54	0.97	0.12	1.7	52
P	121	R	105	R	105	R	123	0.98	0.05	4.7	14
E	181	E	157	F	157	S	177	0.89	0.10	2.45	42
N	182	I	158	L	158	L	178	0.78	0.09	2.1	42
G	183	D	159	T	159	P	179	0.97	0.08	1.28	42
E	184	E	160	G	160	S	180	0.80	0.06	3.26	42
S	450	G	312	N	307	N	331	0.33	0.12	1.68	51

ⁱ, no citation indicates new data; ⁻, no phi estimate (see Methods); NF, non-functional mutants; agonist phi is $\geq 0.93^{13,53}$.

Supplementary References

- 45 Purohit, P., Bruhova, I. & Auerbach, A. Sources of energy for gating by neurotransmitters in acetylcholine receptor channels. *Proceedings of the National Academy of Sciences* **109**, 9384-9389, doi:10.1073/pnas.1203633109 (2012).
- 46 Chakrapani, S., Bailey, T. D. & Auerbach, A. The role of Loop 5 in acetylcholine receptor channel gating. *J. Gen. Physiol.* **122**, 521-539 (2003).
- 47 Purohit, P. & Auerbach, A. Acetylcholine Receptor Gating: Movement in the α -Subunit Extracellular Domain. *J. Gen. Physiol.* **130**, 569-579 (2007).
- 48 Purohit, P. & Auerbach, A. Glycine Hinges with Opposing Actions at the Acetylcholine Receptor-Channel Transmitter Binding Site. *Molecular pharmacology* **79**, 351-359 (2011).
- 49 Mitra, A., Cymes, G. D. & Auerbach, A. Dynamics of the acetylcholine receptor pore at the gating transition state. *Proc. Natl Acad. Sci. USA* **102**, 15069-15074 (2005).
- 50 Cadugan, D. J. & Auerbach, A. Conformational dynamics of the alphaM3 transmembrane helix during acetylcholine receptor channel gating. *Biophys J* **93**, 859-865, doi:10.1529/biophysj.107.105171 (2007).
- 51 Mitra, A., Bailey, T. D. & Auerbach, A. L. Structural dynamics of the M4 transmembrane segment during acetylcholine receptor gating. *Structure* **12**, 1909 (2004).
- 52 Bafna, P. A., Jha, A. & Auerbach, A. Aromatic Residues ϵ Trp-55 and δ Trp-57 and the Activation of Acetylcholine Receptor Channels. *J Biol Chem* **284**, 8582-8588 (2009).
- 53 Grosman, C., Zhou, M. & Auerbach, A. Mapping the conformational wave of acetylcholine receptor channel gating. *Nature* **403**, 773 (2000).
- 54 Jha, A. & Auerbach, A. Acetylcholine receptor channels activated by a single agonist molecule. *Biophys J* **98**, 1840-1846 (2010).
- 55 Sigg, D., Bezanilla, F. & Stefani, E. Fast gating in the Shaker K⁺ channel and the energy landscape of activation. *Proc Natl Acad Sci U S A* **100**, 7611-7615, doi:10.1073/pnas.1332409100 (2003).